Available online at www.HighTechJournal.org

HighTech and Innovation Journal

ISSN: 2723-9535

Vol. 5, No. 2, June, 2024

# Analysis of Seasonal Wind Energy Potential on Zanzibar Coastal Island

Buruhan Haji Shame [1, 3], Dominicus D. D. P. Tjahjana [1], Ubaidillah [1, 2*], Muhammad Aziz [4], Manala T. Mbumba [5]

[1] *Graduate School of Engineering, Sebelas Maret University, Surakarta, 57126, Indonesia.*

[2] *Mechanical Engineering Department, Islamic University of Madinah Al Munawwarah, Madinah, 42351, Saudi Arabia.*

[3] *The Ministry of Infrastructure, Communication and Transportation, Zanzibar, 71202, Tanzania.*

[4] *The Institute of Industrial Science, University of Tokyo, Tokyo, 113-0033, Japan.*

[5] *Department of Transport Engineering and Technology, National Institute of Transport, Dar es Salaam, 255, Tanzania.*

Received 30 January 2024; Revised 22 April 2024; Accepted 07 May 2024; Published 01 June 2024

**Abstract**

The main objectives of this research were to numerically analyze the potential for seasonal wind power (WP), assess wind direction, and select the most effective wind turbine (WT) for installation at the research site. Wind data were collected half-hourly from a branch of the Tanzania Meteorological Authority nearest to the research site. The collected data were analyzed using a double-parameter Weibull distribution (WD) model, where the standard deviation (SD) method was used to fit the WD. The results revealed that the site experienced strong winds within the range of 4.5–7 m/s between the hours of 05:00 - 20:00, with the most likely seasonal wind speed (WS) ranging from 5–7 m/s, while the mean seasonal WS was 9.07–12.14 m/s. The highest possible wind energy density (wED) of 23.3 GWh/m$^2$ at a hub height of 10 m occurred during winter, followed by spring, autumn, and summer, with 6.39, 6.32, and 3.33 GWh/m$^2$, respectively. The annual wED was > 13.52 GWh/m$^2$, with a typical month-to-month energy of 1.13 GWh/m$^2$. Finally, the study concluded that the recommended WT model (POLARIS P62-1000) was the best choice for installation at the study site due to its sustainable WS and WP potential. Based on the findings of this research, which show that the site has sustainable seasonal wind resources, it is suggested that future wind research be carried out to extend the dataset to ensure the long-term seasonal wind pattern at the site.

*Keywords:* Weibull Distribution; Wind Energy; Energy Analyss; Renewable Energy; Zanzibar.

## 1. Introduction

Sustainable energy resources have been instrumental in addressing the issue of planetary warming, which has been causing harm to the natural environment [1–3]. To address the detrimental environmental consequences associated with conventional energy sources and to meet the increasing global energy demand, there has been a notable focus on researching renewable energy options in various interdisciplinary environmental and engineering investigations [4–8]. Among these sustainable energy sources, wind power (WP) stands out as a remarkably valuable and promising selection. Wind power (WP) is inherently clean, readily available, cost-effective, sustainable, and eco-friendly [6, 9–11].

Wind power (WP) is swiftly emerging as the preferred option for sustainable energy in both advanced and emerging economies, owing to its myriad advantages [12–14]. For example, nations like Denmark, Spain, Germany, the United

* Corresponding author: ubaidillah_ft@staff.uns.ac.id

http://dx.doi.org/10.28991/HIJ-2024-05-02-08

States of America, China, and India rely heavily on WP as their primary source for the generation of electricity. For example, nations like Denmark, Spain, Germany, the United States of America, China, and India rely heavily on WP as their primary source for the generation of electricity [15]. Remarkably, the global collective mounted capacity of WP has been consistently and rapidly increasing [16–19]. Egypt, Morocco, and Tunisia hold notable positions in the realm of WP within Africa, with connected capacities reaching 550, 291, and 114 MW, respectively, by the end of 2011 [20]. The growing energy demand, the rapid exhaustion of non-renewable energy reserves, and environmental concerns associated with their utilization have resulted in the pursuit and establishment of primary energy sources, like WP, for electricity generation [21–23]. Due to variations in climatic conditions, several studies had to be conducted to determine the adequacy and sustainability of WP as a fundamental step towards the selection of wind farm (WF) sites.

In their research, Ongaki et al. investigated the prospects of WP in Kiisi, Kenya, utilizing both the Weibull distribution (WD) and Rayleigh distribution methods [24]. The moment system was employed to continuously calculate the WD parameters over a 10-year period spanning 2004–2013. Their study revealed a decreasing trend in wind speeds (WSs) over time and emphasized that WP during the winter exceeded that of the summer [21]. This fluctuation in WP was attributed to the direct relationship between WS and atmospheric density [25, 26]. In the Kiisi region, during the cold season, the atmospheric density was observed to be greater than during the warm season, primarily due to heightened atmospheric moisture content [27]. Based on their findings, the authors concluded that the wind energy density (wED) in the Kiisi region was sufficient for a variety of off-grid electrical and mechanical applications, including battery charging, the operation of small wind generators, and water pumps for domestic, industrial, and agricultural purposes [28–30].

Jowder [31] analyzed wind data spanning three years in the Kingdom of Bahrain using the WD function. The study indicated that the selected sites were suitable for the installation of small-scale wind turbines (WTs) at a height of 30 m and large-scale WTs at a height of 60 m. Awad [32] conducted in the Zafarana area of Egypt, the Weibull distribution function was utilized along with methods such as Mean Squared Deviation (MSD), Maximum Likelihood (ML), Genetic Algorithm (GM), Probability Distribution (PD), and Modified Maximum Likelihood (MML) to analyze one year of wind data. Additionally, the data collected at 10-minute intervals for one day each in summer and winter were examined. The performance of these methods was assessed using the root mean square error (RMSE). The study recommended the use of MSD and ML for estimating the wind potential. Furthermore, in a separate investigation, five distinct geographical regions worldwide were analyzed using 96 months of wind data [33]. Five distinct geographic regions worldwide were analyzed using 96 months of wind data. Instead of relying on the measured data, the study employed the WD function to determine the approximate wind potential in these areas.

Katinas conducted an assessment of the efficiency of breeze energy in the context of installed WTs, employing the capacity factor (CP) as a key metric for the WS assessment at more than 18 sites in Lithuania [34]. The chi-square, constant of determination, and error methods were employed to validate the best method of analysis between the ML, MML, and wasp algorithms, whereby the WAsP algorithm and extreme likelihood were found to have the best fits for the WD compared to the modified extreme likelihood method [35, 36]. The wasp algorithm was used to estimate the wED. A technical assessment of electricity production was also conducted, which involved the analysis of three commercial WTs by calculating and comparing the average power (AP) and performance of the selected WTs. The study concluded that the sites had high WSs, making them suitable for the installation of WTs [37].

Michael et al. assessed the WP potential along the Dar es Salaam coastline. Their approach involved employing graphical representations and the standard deviation (SD) method to determine the WD parameters [38]. From the results of the study, the SD method proved to be the most appropriate method for evaluating the WP potential in that area. Consequently, the researchers recommended that the WD parameters derived via the SD method be adopted when selecting the right commercial WTs. Also, Oyedepo et al. conducted a study that involved analyzing WS data and assessing the WP potential in three specific areas in southeast Nigeria. The WD and SD models were employed to calculate the WD parameters [39]. The findings of the study revealed that the average WSs in these three locations fell within the range of 3.3–5.4 m/s. Subsequently, the annual energy output and the most suitable WTs were selected for each of the study locations in southeast Nigeria [40, 41].

Zanzibar, an archipelago located in East Africa and surrounded by the Indian Ocean, boasts abundant renewable energy resources such as wind, oceanic tides, solar, and geothermal energy. However, despite this wealth of resources, the island relies heavily on external sources for its electricity supply, mainly due to its connection to Tanzania's primary grid through an underwater cable [42, 43]. Ensuring a consistent power supply presents a significant challenge, especially during the dry season when fluctuations in water levels in the hydropower reservoir disrupt the generation of electricity from Tanzania's main grid [44]. Furthermore, concerns about infrastructural issues related to the submarine cable responsible for transmitting power to the island play a crucial role [18].

The existing research conducted in various regions, including Kenya, Bahrain, Egypt, Lithuania, and Nigeria, has contributed valuable insights into wind resource assessment methodologies and WT suitability. However, there is a research gap in the understanding of wind characteristics and wind potential in Zanzibar, Tanzania, due to a lack of

literature specifically written to assess the wind potential at the study site. Existing studies primarily utilized methods such as the WD function to analyze wind data and estimate WP potential, but none directly addressed the unique wind patterns and atmospheric conditions prevalent in Zanzibar. Therefore, a new research endeavor in Zanzibar would provide tailored insights into the feasibility of seasonal WP and the selection of the WT to be installed at the study site for this research. The study used the Weibull distribution (WD) method, with the best fit by the SD method, to analyze the seasonal wind patterns and energy potential at the study site.

## 2. Data Acquisition and Study Site

The data on WS and direction utilized in this study were gathered from the Zanzibar station of the Tanzania Meteorological Authority. This data was collected at 30-minute intervals throughout the entire year (January–December 2022). The measurements were obtained at a height of 10 m above ground, with the study location being at an elevation of 18 m at coordinates (6°13'S, 39°13'E). Figure 1 shows the geographical location of the study area. The study area experiences four separate climatic seasons: spring (March–May), summer (June–August), autumn (September–November), and winter (December–February) [18].


**Figure 1. Geographical location of the study site**

## 3. Research Processes

The research processes refer to the systematic approach undertaken to investigate, explore, and discover new knowledge or to deepen understanding within a particular field or topic of interest, including the concern of this study. It typically involves a series of steps, which may include defining the research question or hypothesis, conducting a review of existing literature, designing a methodology or research plan, collecting and analyzing data, interpreting findings, and drawing conclusions. Figure 2 shows the methodology flow chart for all processes applied in this research. The methodology flow chart for this study (Figure 2) entailed a systematic approach to analyzing the wind data and assessing the seasonal WP potential at the study site.

Initially, the wind data, which was collected half-hourly from the Tanzania Meteorological Authority, served as the foundational dataset for subsequent analyses. Following the data collection, the analysis progressed to an examination of the daily wind profiles for each season to discern seasonal variations in wind patterns. Concurrently, a comprehensive wind direction analysis was conducted to determine prevailing wind patterns and their variability over time. A basic analysis was done, whereby a Weibull distribution (WD) model fitted to the collected wind data using the standard deviation (SD) method facilitated the characterization of the PD of WSs at the study location.

The model was further refined by determining the Weibull distribution (WD) parameters, thus enabling a more precise assessment to be made of variations in the WS. This analysis was a key step in understanding the reliability and consistency of wind resources, ultimately contributing to the calculation of the wind power (WP) potential and wind energy density (wED). Additionally, the study incorporated the wind sustainability classification of the National Renewable Energy Laboratory (NREL) to evaluate the sustainability of the wind resource. Furthermore, seven different WT models were analyzed to assess their performance in the given wind conditions, culminating in the selection of the most suitable WT. The methodology flow chart concluded with a discussion of the findings and limitations of the study, providing insights into the results obtained and addressing any challenges encountered during the research process, followed by a concise conclusion summarizing the key outcomes of the study.

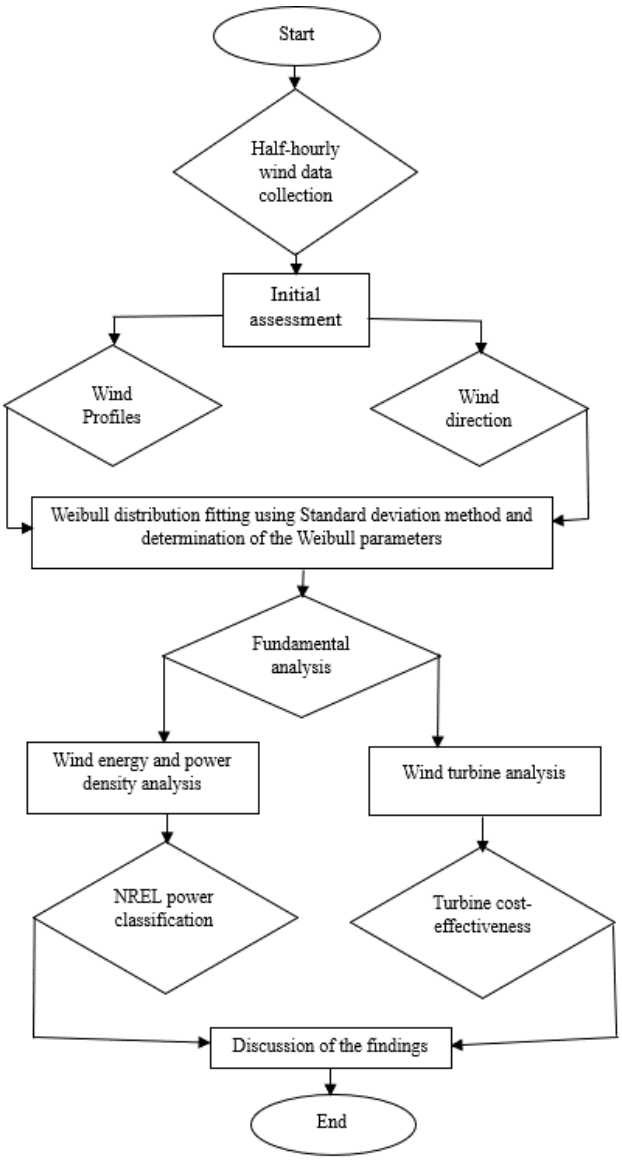


**Figure 2. Research methodology flowchart**

## 4. Data Analysis and Mathematical Models

This research employed the two-factor Weibull distribution (TWD). TWD is the most effective method that has been used to analyze wind data. It has two fundamental functions, namely the likelihood function as given in Equation 1 and the increasing function as given in Equation 2 [45–48]. Whereas c and k are the unknown variables, namely the scale constant in m/s and the non-dimensional shape constant of the distribution, respectively, and *v* is the recorded wind speed in m/s [49].

$$f(v) = \left(\frac{k}{c}\right)\left(\frac{v}{c}\right)^{k-1} exp\left(-\frac{v}{c}\right)^{k} \quad (1)$$

$$F(v) = 1 - exp\left(-\frac{v}{c}\right)^{k} \quad (2)$$

In this study, the values of these constants were determined using standard deviation method as per as Equations 3 and 4 [46], $\sigma$ and $\bar{v}$ are the respective standard deviation of the wind speed and average wind speed in m/s.

$$k = \left(\frac{\sigma}{\bar{v}}\right)^{-1.086} \quad (3)$$

$$c = \frac{\overline{v}}{\Gamma\left(1+\frac{1}{k}\right)} \quad (4)$$

The gamma function $\Gamma$ was calculated using Equation 5 [50]:

$$\Gamma(x) = \int_0^{\infty} t^{x-1} e^{t}\, dt \quad (5)$$

From Equation 3, $\sigma$ is the standard deviation of the wind speed given as in Equation 6**,** $n$ is the number of data taken into consideration of the analysis at a given time, $v_i$ is the actual velocity at time step $i$ and n[th] record, $\bar{v}$ serves as the average velocity given in Equation 7 [51].

$$\sigma = \sqrt{\left(\frac{1}{n}\sum_{i=1}^{n}(v_i - \bar{v})^2\right)} \quad (6)$$

$$\bar{v} = \frac{1}{n}\sum_{i=}^{n} v_i \quad (7)$$

Equation 8 determines a particular speed denoted as $v_m$ at which maximum energy generation can be achieved while the maximum attainable speed of the wind, represented as $v_p$ (m/s) is given by Equation 9, $c$ and $k$ are the determined Weibull scale and shape factor of the distribution respectively [52, 53].

$$v_m = c\Gamma\left(\frac{k+2}{k}\right)^{\frac{1}{k}} \quad (8)$$

$$v_p = c\Gamma\left(\frac{k-1}{k}\right)^{\frac{1}{k}} \quad (9)$$

### 4.1. Wind Power and Energy Density

At any airstream speed $v$ in m/s, the wind power concentration in W/m$^2$ is given as per as Equation 10 whereas the corresponding energy concentration in kWh/m$^2$ was calculated using Equation 11 [54]**:**

$$\frac{P}{A} = \int_0^{\infty}\frac{1}{2}\rho v^3 f(v)dv = \frac{1}{2}\rho c^3\Gamma\left(\frac{k+3}{k}\right) \quad (10)$$

$$\frac{P}{A} = \int_0^{\infty}\frac{1}{2}\rho T v^3 f(v)dv = \frac{1}{2}\rho c^3\Gamma\left(\frac{k+3}{k}\right)T \quad (11)$$

From the recently mentioned Equations 10 and 11, A represents the area of the turbine in m², while P and E denote the respective airstream power and energy concentrations. ρ represents the atmospheric density, ideally taken as 1.225 kg/m³. T indicates the period of time for the analysis, and c and k are the respective constant factors of the distribution [54].

### 4.2. Extrapolation of the Constants of Distribution

Extrapolation of the Weibull parameters is one of the important techniques used during the analysis of airstream speed variation with the height of the turbine. If $k_0$ is the initial non-dimensional shape factor at any initial hub height $h_0$, and a projected height $h$ is given, then the shape constant at the projected height k(h) is given as shown in Equation 12 [39, 55].

$$k(h) = k_0\frac{\left[1\text{-}0.088\ln\left(\frac{h_0}{10}\right)\right]}{\left[1\text{-}0.088\ln\left(\frac{h}{10}\right)\right]} \quad (12)$$

Similarly, the projected scale constant *c(h)* at any given projected height $h$ was calculated using Equation 13, if $c_0$ is the initial scale factor at 10-meter height [56].

$$c(h) = c_0\left(\frac{h}{h_0}\right)^n \quad (13)$$

Since $c_0$ and $h_0$ are the initial scale constant and height in respectively, then the value of $n$ was calculated using Equation 14 of this research [57];

$$n = \frac{[0.37 - 0.088\,ln(c_0)]}{\left[1 - 0.088\,ln\left(\frac{h}{10}\right)\right]} \quad (14)$$

In this study, initial hub height $h_0$ was 10 meters above the ground as described in the data source section of this research.

### 4.3. Wind Turbine Performance Analysis

An effectiveness analysis of the wind turbine can be measured using two fundamental factors, these are the generated output as well as capacity or performance factor [50, 58, 59]. With turbine activation speed $v_c$ , optimal speed $v_f$, rated or halt speed of the wing $v_r$, design power $P_{eR}$ in kW, the average generated output $P_{e,ave}$ of the turbine is given as Equation 15 [39].

$$P_{e,\ ave} = P_{eR}\left(\frac{e^{-\left(\frac{v_c}{c}\right)^k} - e^{-\left(\frac{v_r}{c}\right)^k}}{\left(\frac{v_r}{c}\right)^k - \left(\frac{v_f}{c}\right)^k}\right) - P_{eR}^{e^{-\left(\frac{v_f}{c}\right)^k}} \quad (15)$$

If the average wind speed $\bar{v}$ is considered, then the average generated output can be calculated using Equation 16 [59].

$$P_{e,\ ave} = \begin{cases} 0 \\ P_{eR}\left(\frac{\bar{v}^k - v_c^k}{v_r^k - v_c^k}\right) \\ P_{eR} \\ 0 \end{cases} for \begin{bmatrix} \bar{v} < v_c \\ v_c \le \bar{v} \le v_r \\ v_r \le \bar{v} \le v_f \\ v_f < \bar{v} \end{bmatrix} \quad (16)$$

In any study, $v_c$, $v_f$ , and $v_r$ are the activating speed, cutout speed, and optimal speed in m/s respectively. For the selected turbine models in any analysis, all parameters in equation 15 and 16 must be given as specification, $c$ and $k$ are the determined Weibull parameters of the distribution. Once the average power is computed using the most suitable Weibull parameters, the capacity factor can be calculated using Equation 17, whereas $C_f$ is the capacity factor of the turbine [60]. To ensure cost-effectiveness, the capacity factor must exceed 0.25 [39].

$$C_f = \left(\frac{P_{e,\ ave}}{P_{wR}}\right) \quad (17)$$

The capacity factor represents the ability of a turbine to transform accessible wind energy into electrical power, with a higher factor indicating reliability and productivity. A comprehensive assessment of both factors ensures optimal performance and economic viability for sustainable energy production.

## 5. Results

The results of this research included the daily wind speed (WS) profiles for all the seasons of the year, seasonal wind classes and directions, WD parameters, WS distributions, WS variations, WP, and wED, and an analysis of seven different WTs, followed by the selection of the highest-performing WT to be installed at the site.

### 5.1. Wind Speed Profile

The mean WS throughout a 24-hour period at a specific location signifies the daily average speed within a season. The study involved calculating the mean WS from all the recorded WSs at 30-minute intervals across 24 hours each day to establish the average daily profile from the dataset. This computation spanned various time segments, such as from 00:00–00:30, 01:30–02:00, and so on. Figure 3 depicts the daily WS profiles of the different climatic seasons observed at the study site.

Throughout all the seasons, robust wind velocities persisted from 05:00–20:00. The WS was 4 m/s at 05:00, which then ascended to a peak of nearly 7 m/s around 15:00, and gradually declined to 3 m/s by 20:00. This observation indicated a sustained period of formidable winds lasting approximately 15 hours daily, totaling 1350 hrs/season and 5400 hrs/year. Strong winds were prevalent across all the seasons. Likewise, the monthly WS profiles exhibited similar fluctuations as observed in the seasonal wind profiles. Robust winds persisted from 05:00 - 20:00 throughout all the seasons, with speeds ranging from 4–8 m/s.

Based on the seasonal wind patterns and the duration of wind fluctuations, the site seemed to have strong WP starting at the beginning of 05:00 and gradually increasing to the peak point at 12:30 and then decreasing towards the minimum expected power at 20:00. The smallest expected power was harvested between 00:00 and 04:40, as well as between 09:00–00:00. These results indicated that a large power output can be expected for more than 5400 hours at the study site, and the enhanced WP and energy stability at the study site make it suitable for the establishment of small to large wind farms.

### 5.2. Seasonal Wind Classes and Direction

A wind rose is a graphical aid used by meteorologists to provide a concise depiction of the typical distribution of WS and direction at a specific location. The seasonal wind directions are illustrated by the wind rose depicted in Figure 4. Typically, in an analysis of wind data, it is important to accurately predict wind direction, particularly when strategizing the installation and micro-siting of a WT or WF. The seasonal wind rose was generated using WRPLOT version 7.0.0.

In the southern (S) direction, wind frequencies fluctuated at 23% in spring, 24% in summer, and 6.5% in autumn. Southwest (SW) winds showed frequencies of 13% in spring, 8% in summer, and 4% in autumn. Similarly, south-southwest (SSW) winds had frequencies of 8% in spring, 7% in summer, and 2.7% in autumn. Notably, there were no winds from the S, SW, or SSW in the winter. Summer witnessed 18% of winds from the southeast (SE) and 8% in autumn. Frequencies of about 7% in autumn and 14.5% in winter were observed in the northern direction (N), while fewer northeast (NE) winds were experienced, with 3% in autumn and 12% in winter. Winter notably experienced a frequency of 6% in wind direction, in contrast to 0% in spring and summer. Wind flow from the east (E) was scarce, comprising only 2% in the autumn and less than 3% in the winter.

The results showed that the expected wED in spring, summer, and autumn was dominated by winds blowing from the southerly direction of the Zanzibar coastal zone, while in winter, the wED was concentrated in the northerly direction

of the study area. In this case, the design of WTs should consider the dominant wind directions in each season. For example, in spring, summer, and autumn, when the wED is dominated by winds from the south, WTs should be oriented to face south to maximize the capture of energy. Yaw control systems in the designed WTs can enable them to rotate and align with changing wind directions to optimize the capture of energy. Knowledge of the dominant wind directions in each season can help optimize the yaw control strategy to ensure WTs are always facing the prevailing winds.

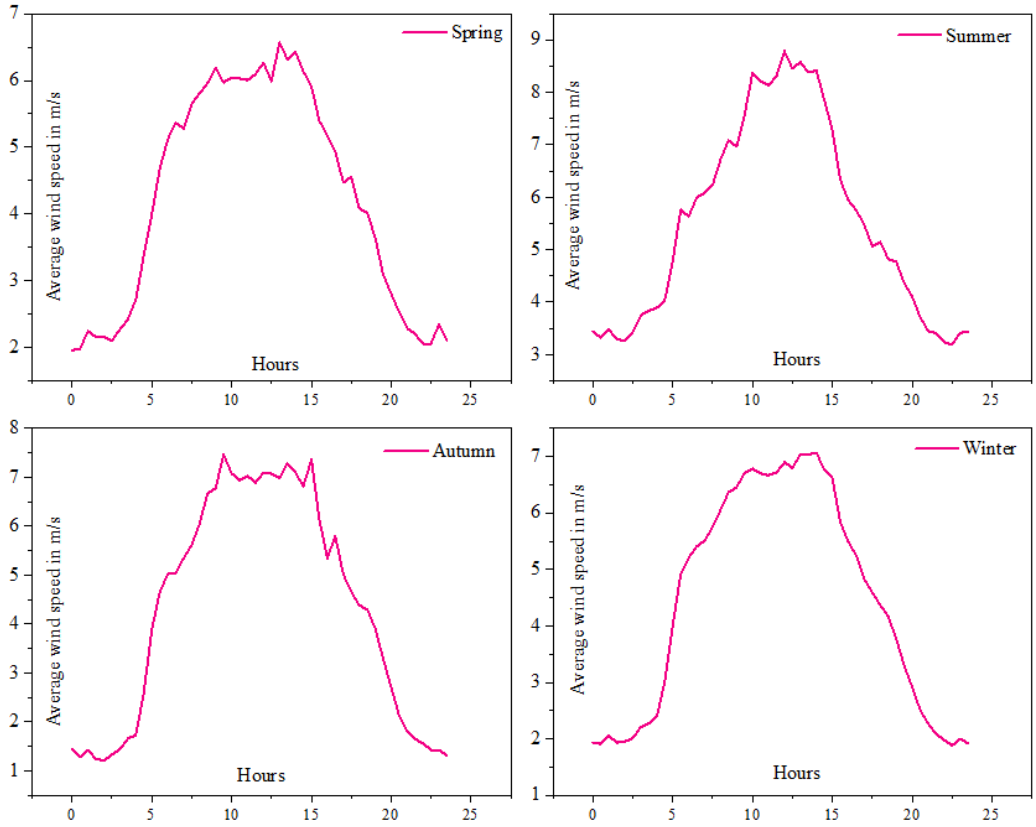


**Figure 3. Daily average wind speed for all seasons of the year**

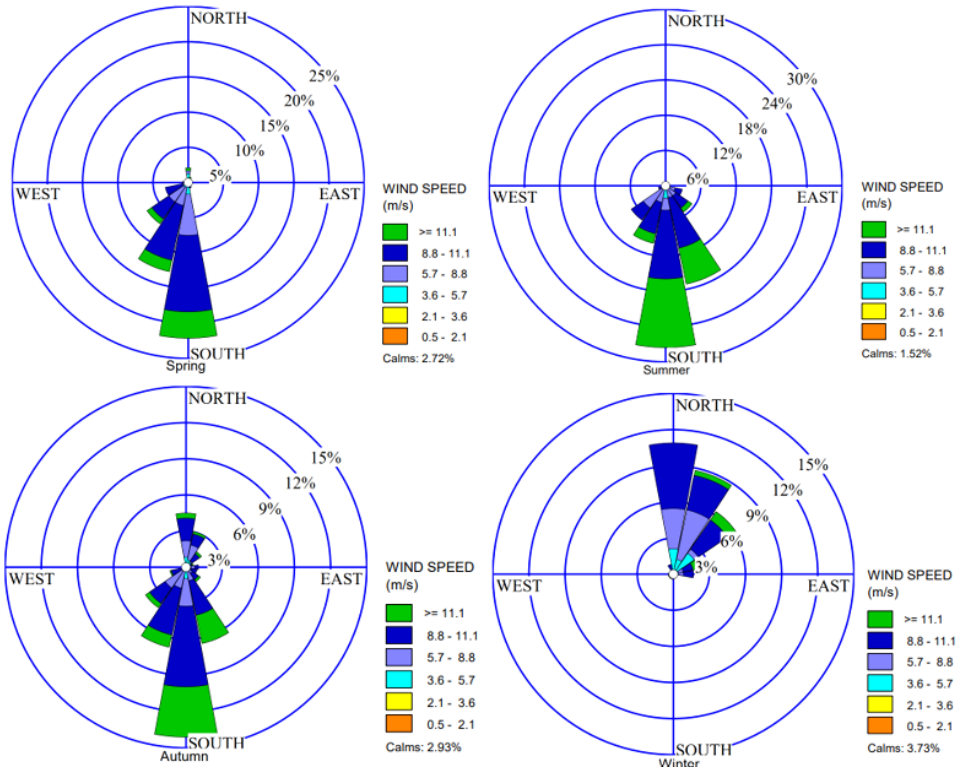


**Figure 4. Wind direction for all seasons of the year**

### 5.3. Weibull Parameters

The shape ($k$) parameter serves as a gauge of wind constancy and the distribution of WSs at a specific location, while the scale ($c$) parameter indicates the wind strength at that site. When $k < 1$, it indicates a higher likelihood of low WSs being observed with very few occurrences of high WSs, reflecting sub-exponential characteristics. If $k = 1$, it implies a constant failure rate or a uniform WS distribution, and if $k > 1$, it signifies a super-exponential rate, meaning that higher WSs are more likely to occur compared to lower WSs. Table 1 clearly shows that the site experienced super-exponential characteristics.

The WD constraints for the entire year in this study were computed using the SD method, resulting in k = 1.62 and $c$ = 11.22 m/s. The monthly WD parameters are provided in Table 1. The findings indicated that March and April had the highest $k$ (2.6 and 2.2, respectively), while April had the largest $c$ (18.04 m/s), followed by May (17.67 m/s).

The seasonal $k$ and $c$ values were assessed for each season (Table 1). The highest $k$ was 1.59 in spring, while the lowest was 1.54 in winter. Additionally, the $k$ values for summer and autumn were 1.57 and 1.55, respectively. In contrast, the $c$ value was computed as 13.53, 12.66, 10.94, and 10.07 m/s for spring, summer, autumn, and winter, respectively, indicating an increase in wind strength over the year. Both the $k$ and $c$ values indicated a significant potential for high WP generation at the site, confirming the presence of strong and stable or super-exponential winds.

There were slightly higher $k$ and $c$ factors, indicating a wider range of WSs in each month and climatic season at the study site. This suggested a more pronounced skewness in the WS distribution, implying periods of significantly higher WSs than average in different climatic seasons. Due to the indicated ranges of the $k$ and $c$ factors in this research, the selected WTs must be designed to capture energy efficiently across a range of WSs, including during periods of higher WSs. This is very important because the larger WD factors could result in increased energy generation during these periods. Also, the site requires WTs to operate efficiently across this broader range to maximize energy generation. Also, WTs designed for this region should incorporate adaptive rotor blade designs and control systems to optimize the capture of energy across varying wind conditions while ensuring that the structural components can withstand the associated stresses.

**Table 1. Monthly and seasonal Weibull parameters**

| Seasons | k | c(m/s) | Months | k | c (m/s) |
|---|---|---|---|---|---|
| Spring | 1.59 | 13.53 | 1 | 2.00 | 12.00 |
| | | | 2 | 1.55 | 10.94 |
| | | | 3 | 2.60 | 12.80 |
| Summer | 1.57 | 12.66 | 4 | 2.20 | 18.04 |
| | | | 5 | 1.50 | 17.67 |
| | | | 6 | 1.50 | 10.03 |
| Autumn | 1.55 | 10.94 | 7 | 2.14 | 9.00 |
| | | | 8 | 1.60 | 10.73 |
| | | | 9 | 2.00 | 9.00 |
| Winter | 1.54 | 10.07 | 10 | 1.02 | 12.00 |
| | | | 11 | 1.60 | 13.53 |
| | | | 12 | 2.00 | 11.8 |

### 5.4. Wind Speed Frequency Distribution

The speed frequency density function (PDF) serves as an illustration of the likelihood of specific WSs occurring at a particular location over time. The PDF showed that its peaks were predominantly skewed toward higher-average WSs. It is worth emphasizing that the highest point on the PDF curve corresponds to the WS that occurs most frequently.

A detailed examination of the curve in Figure 5(a) revealed that the most common WS in 2022 was 8 mm/s (70% occurrence). Furthermore, the annual PDF underscored that in 2022, a broader spectrum of WSs was expected, with a noticeable inclination towards higher WSs. The increasing PD of the WS at the research site, represented by the curve in Figure 5(b), exhibited a comparable pattern. The cumulative distribution function is a valuable tool for approximating the duration during which WSs fall within a specific speed range. When considering that a WS of $\geq$ 2.5 m/s is required to activate a WT, it was evident that the site experienced frequencies of approximately 99.9% throughout 2022.

Concerning the seasonal WS frequencies, the peak WS in all seasons ranged between 5–6.8 m/s, with frequencies ranging between 58–76%. This was attributed to its larger $k$ and $c$ values. The ranking in descending order was spring, summer, autumn, and winter, with progressively diminishing super-exponential rates. In terms of the seasonal cumulative distribution at a cut-in speed of 2.5 m/s, the site recorded a frequency of approximately 99.55% in spring,

99.72% in summer, 99.92% in autumn, and 99.96% in winter. As stated by Oyedepo et al. [39], if a WT with an activation speed of 2.2 m/s is employed to harness WP for electricity generation, the site would achieve cumulative frequencies surpassing 92%. Consequently, the site demonstrated a notable inclination towards wind fluctuations, as evidenced by both the annual and seasonal cumulative frequencies, which exceeded 92% at a minimum WS of 2.2 m/s.

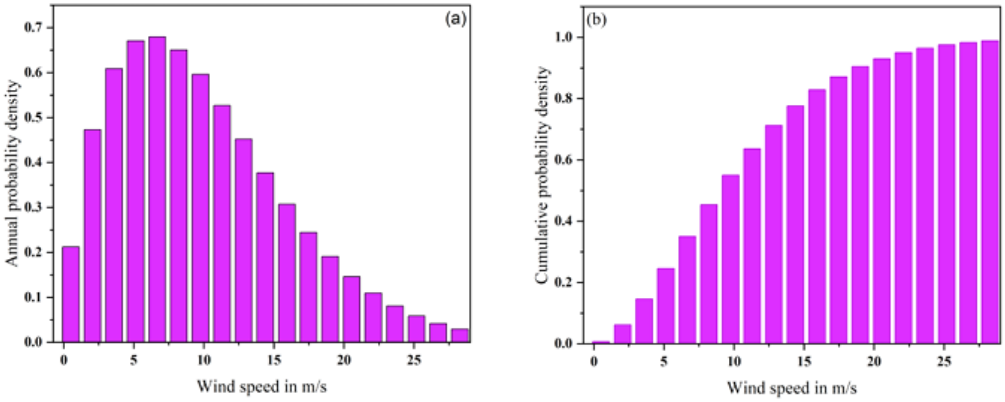


**Figure 5. Annual wind speed distribution**

## 5.5. Wind Speed Variation

The monthly average WS variations are shown by the blue bars in Figure 6. April and May stood out as the months with the highest average WS (15.97 m/s). October and November exhibited an equal average WS (12.14 m/s), while the lowest average WS (8.3 m/s) was observed in July and September. The results showed that all the months had high WSs, indicating overall that wind resources were available at the study site. Also, these average WSs meant that there was more kinetic energy available in the wind, which could be harnessed by WTs to generate electricity. This is the most essential factor for determining the potential energy production capacity of a WF or WT.

The most probable WSs, which represented the WSs with the highest likelihood of occurrence in each month, are shown by the dark green bars in Figure 6. The finding emphasized that the most probable WS for a given month reached its maximum (13.71 m/s) in April, differing from other months, which had the most frequent speeds ranging between 3–9 m/s. Excluding October, the month with the smallest count was February (3 m/s), followed by June and July (4.5 m/s). October experienced a most probable WS of 0.206 m/s, which was associated with a sub-exponential rate defined by a *k* factor of 1.02 (Table 1). The results showed that more than 80% of all the months had the most frequent WSs of > 4.5 m/s. This indicated a greater likelihood of consistent energy generation, making the location more favorable for WP projects.

Furthermore, the maximum WS ranged from 12–36 m/s (Figure 6; red bars). These results indicated the consistent presence of strong and enduring wind conditions at the research site on a monthly basis. Large maximum speeds of >15 m/s are likely to occur a few times a month and can sometimes cause natural disasters. While WTs are designed to withstand a certain range of WSs, extreme gusts beyond the design limits can pose challenges and potential risks to the structural integrity and operational stability of the WTs.

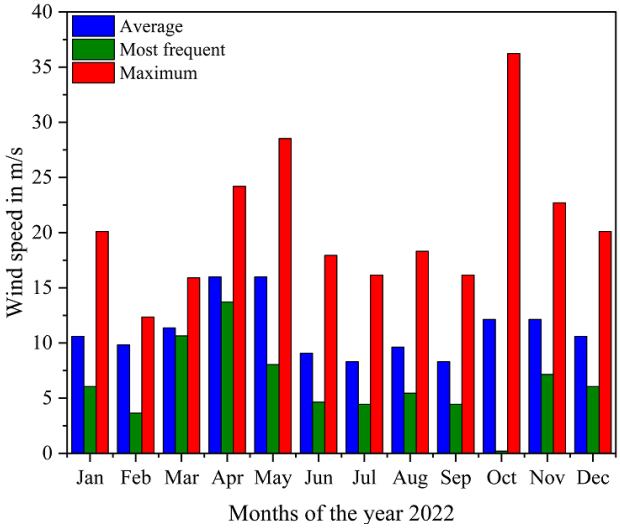


**Figure 6. Disparity of the monthly wind speed**

In the case of seasonal variations in WSs, the results of this investigation revealed that throughout the span of a year, the average WS was measured within the interval of 10.06–12.14 m/s. The summer season had the smallest average WS, while the largest average WS was observed during spring and autumn (Table 2). The most probable seasonal WS ranged between 5.53 m/s (summer) and 6.74 m/s (spring and autumn), with winter recording a maximum WS of 5.6 m/s. The maximum seasonal WSs observed ranged between 18–23.28 m/s (Table 2). These results showed that the site also has sustainable seasonal wind fluctuations, which provides a scientific argument for high expected WP generation.

**Table 2. Seasonal wind speed variation**

| Seasons | $\bar{v}$ (m/s) | $v_p$ (m/s) | $v_m$ (m/s) |
|---|---|---|---|
| Spring | 12.136 | 6.734 | 23.279 |
| Summer | 9.835 | 5.531 | 18.763 |
| Autumn | 12.136 | 6.734 | 23.279 |
| Winter | 10.601 | 5.644 | 20.661 |

## 5.6. Wind Power and Energy Variation

The yearly WP at the site for 2022 was calculated to be 1543.035 W/m², which is equivalent to 13.52 GWh/m². This indicated that the location was characterized by relatively strong and consistent wind conditions, making it favorable for WP generation. Also, the calculated yearly WP and wED provided valuable insight into the average wind resource available at the site over the course of the year, which was high. Wind turbines (WTs) must be designed to efficiently capture and convert this WP into electricity, resulting in higher overall energy production from the WF. Table 3 shows the seasonal and monthly wEDs and wind power densities (wPDs) at the study site.

The results showed that there was a sustainable monthly and seasonal wPD and wED at the site. In spring, the wPD was 2892.911 W/m$^2$ with a wED of 6387.547 MWh/m². In summer, the wPD decreased to 1524.689 W/m$^2$ with a wED of 3329.921 MWh/m². Autumn saw a return to a wPD of 2892.911 W/m$^2$, matching a wED of 6318.117 MWh/m². Winter exhibited the highest wPD (10806.963 W/m$^2$), resulting in a wED of 23343.041 MWh/m². The higher wPD and wED in winter compared to other seasons suggested that winter experienced stronger and more consistent winds, resulting in a greater potential for WP generation during this season. These variations in WP and wED across the seasons highlighted the seasonal fluctuations in WP potential at the site, with winter showing the highest potential for WP generation.

**Table 3. Monthly and seasonal Power and Energy densities**

| Seasons | P(W/m$^2$) | E(MWh/m$^2$) | Months | P(W/m$^2$) | E(MWh/m$^2$.) |
|---|---|---|---|---|---|
| Spring | 2892.911 | 6387.547 | 1 | 1889.736 | 1405.964 |
| | | | 2 | 1505.426 | 1011.646 |
| | | | 3 | 1375.645 | 1023.480 |
| Summer | 1524.689 | 3329.921 | 4 | 4361.021 | 3139.935 |
| | | | 5 | 7048.452 | 5244.049 |
| | | | 6 | 1275.444 | 918.320 |
| Autumn | 2892.911 | 6318.117 | 7 | 459.886 | 706.810 |
| | | | 8 | 1405.541 | 1024.812 |
| | | | 9 | 950.014 | 684.010 |
| Winter | 10806.963 | 23343.041 | 10 | 6511.441 | 4844.512 |
| | | | 11 | 2767.312 | 1992.465 |
| | | | 12 | 1889.736 | 1405.964 |

In analyzing the wPD and wED across the various months, it became evident that certain months stood out with notably high values. May emerged as one of the leading months, boasting a substantial wPD of 7048.452 W/m$^2$ with a wED of 5244.935 MWh/m$^2$, followed closely by October, which recorded a wPD of 6511.441 W/m$^2$ and a wED of 4844.512 MWh/m$^2$. On the contrary, July exhibited the smallest wPD (459.886 W/m$^2$) with a wED of 706.810 MWh/m$^2$, while September followed suit with a wED of 950.014 W/m$^2$. Despite these variations, the data also revealed that the remaining months exhibited commendable wPDs (1200–4261.021 W/m$^2$). Overall, the analysis indicated that over 94% of all the months at the study site experienced substantial WP, attributed to the presence of strong and stable wind fluctuations, while the months with a low wPD experienced excessive humidity or stagnant air masses, which disrupted wind flow.

Since all the WP and wEDs calculated were the result of the WSs recorded at a height of 10 m, the site was expected to have sufficient wind resources because WS generally increases with altitude due to reduced surface friction and increased exposure to atmospheric pressure gradients, thus proving that coastal regions and areas with maritime climates tend to have more consistent and higher WSs compared to inland areas. Therefore, WTs installed at higher altitudes can access stronger and more consistent winds, thereby enhancing the energy potential at the study site.

According to the guidelines on power classification conditions provided by the NREL, a wPD of within 0.0–0.2 kW/m² is low or unsuitable for significant energy generation. Conversely, a wED of 0.8–2.0 kW/m² is preferable for efficient power generation. Further details regarding other wED classes can be found in Table 4. In all the months and seasons of 2022, the wED at the selected site was 10524.69–10806.96 W/m² in a season, while the monthly wED was 459.89–7048.45 W/m² at the 10-meter hub. The seasonal wED was 3329.92–23343.04 MWh/m² and the monthly wED was 706.81–5244.05 MWh/m². Based on these results, it was concluded that the study site had a good range of power sustainability or potentially superb conditions for WP.

**Table 4. NREL Wind power density classification [61]**

| Category | Power interval (kW/m$^2$) | Potential indicator |
|---|---|---|
| 1 | 0 to 0.2 | Unsuitable |
| 2 | 0.2 to 0.3 | Appropriate for Independent use |
| 3 | 0.3 to 0.4 | Decent |
| 4 | 0.4 to 0.5 | Decent |
| 5 | 0.5 to 0.6 | Excellent |
| 6 | 0.6 to 0.8 | Outstanding |
| 7 | 0.8 to 2.0 | Superb |

## 5.7. Performance Analysis of the Turbine Models

It is important to analyze the annual, seasonal as well as monthly performance of wind turbines (WTs) to evaluate their performance, monitor their efficiency, and forecast their energy production. By analyzing their actual power output compared to expected levels, operators can identify WTs that are underperforming and address potential issues to ensure the optimal operation of a wind farm (WF). Additionally, accurate power output data is essential for financial analysis, regulatory compliance, and energy forecasting, enabling energy providers to assess the economic viability of the project, meet regulatory requirements, and manage electricity supply and demand effectively. Overall, it is essential that the power output be calculated annually, seasonally, and monthly to optimize performance, ensure operational efficiency, and meet regulatory and financial objectives in the WP industry.

At the study site, seven commercial WT models with rated powers of 50–1000 kW were selected for the performance simulation (Table 3). These models included the Polaris America LLC models P15-50, P19-100, P50-500, and P62-1000 manufactured in Lakewood, New Jersey; the WES30 model from WP Solutions BV based in the Netherlands; the WWD-1-60 model by Win Wind manufactured in Espoo, Finland; and the BONUS 1000–54 produced by Siemens AG in Erlangen, Germany. Table 5 provides a comprehensive description of the selected WT models along with their distinctive characteristics.

**Table 5. Specifications of selected wind turbines models [38]**

| Parameters | `P15-50 | P19-100 | WES30 | P50-500 | P62-1000 | WWD-1-60 | B-1000-54 |
|---|---|---|---|---|---|---|---|
| Nominal Power (kW) | 50 | 10 | 250 | 500 | 1000 | 1000 | 1000 |
| Tower Height (m) | 30 | 30 | 36 | 50 | 60 | 70 | 45 |
| Blade span (m) | 15.2 | 19.1 | 30 | 50 | 62 | 60 | 54 |
| Starting Wind speed (m/s) | 2.5 | 2.5 | 2.7 | 2.5 | 2.5 | 3.6 | 3 |
| Nominal Wind speed (m/s) | 10 | 12 | 12.5 | 12 | 12 | 12.5 | 14 |
| Ceasing wind speed (m/s) | 25 | 25 | 25 | 25 | 25 | 25 | 25 |

### 5.7.1. Annual and Seasonal Analysis

The annual average power (AP) of the selected WTs was calculated and analyzed. The WT model that generated the highest AP was the POLARIS P62-1000 (589.13 kW), followed by the WWD-1-60 and BONUS B-1000-54 (516.14 and 482.41 kW, respectively). On the other hand, the WTs with the lowest AP were the POLARIS P19-100 and POLARIS P15-50 (5.31 and 28.90 kW, respectively). The AP of the WES30 and POLARIS P50-500 models was 130.19 and 288.08 kW, respectively (Figure 7a). Regarding the annual CP, the POLARIS P62-1000 model achieved the highest CP (0.589; 58.9%), followed closely by both the POLARIS P15 and P50-500 (0.5707; 57.07%). The CP of the POLARIS P19-100,

WES30, and WWD-1-60 models was 53.1, 52.07, and 51.6%, respectively, while the BONUS B-1000-54 model had the lowest CP (48.24%) (Figure 7b).

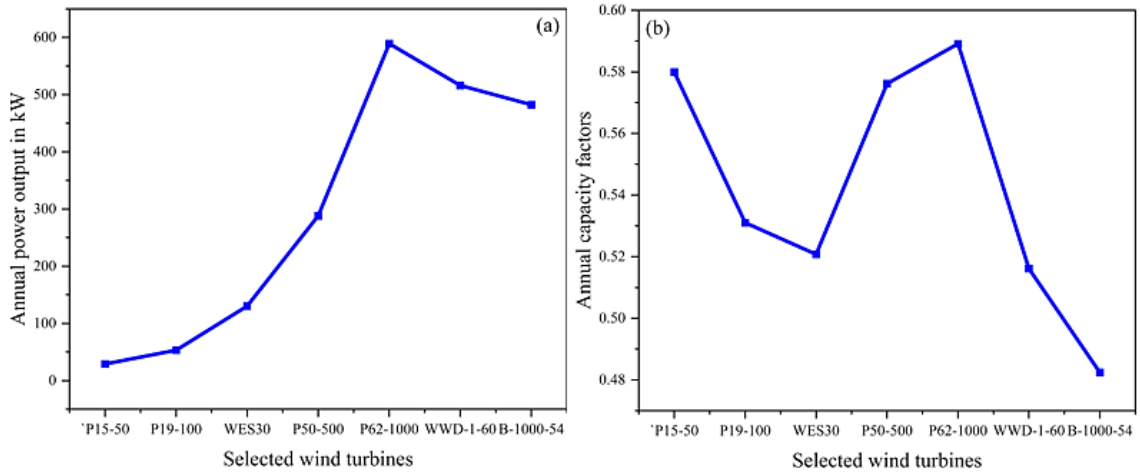


**Figure 7. Annual (a) Turbine power output and (b) Performance of the turbines**

In terms of the seasonal AP, the highest AP was obtained in the spring, summer, autumn, and winter using the POLARIS P62-1000, WWD-1-60, and BONUS B-1000-54 models, respectively. Specifically, all these WT models generated the highest AP during spring, producing approximately 634.6, 614, and 562.4 kW, respectively, followed by 529.7, 492.9, and 465.9 kW, respectively, for summer. Overall, the AP derived from the selected WT models for all the seasons ranged between 28.8–634.6 kW (Figure 8a). The results also demonstrated that the POLARIS P62-1000 had the largest AP.

The findings also indicated that the highest CP for all the WTs (56.24–67.1%) was in the spring, followed by the summer (46.6–58.3%). For autumn and winter, the CP ranged between 47–57.6% and 45.5–56.8%, respectively (Figure 8b). Among all the four seasons, the POLARIS P62-1000 model boasted the highest CP. It is noteworthy that all the selected WT models exhibited a CP of > 25%, indicating their cost-effectiveness. Taking into consideration the annual quarter for the respective months of the season, the results showed that the POLARIS P15-50 had a large CP but a small AP. However, the POLARIS P62-1000 had a large CP that was close to that of the POLARIS P15-50 but had a very large power compared to the P15-50 in all seasons. For this reason, the POLARIS P62-1000 was the best and preferred choice for the study site.

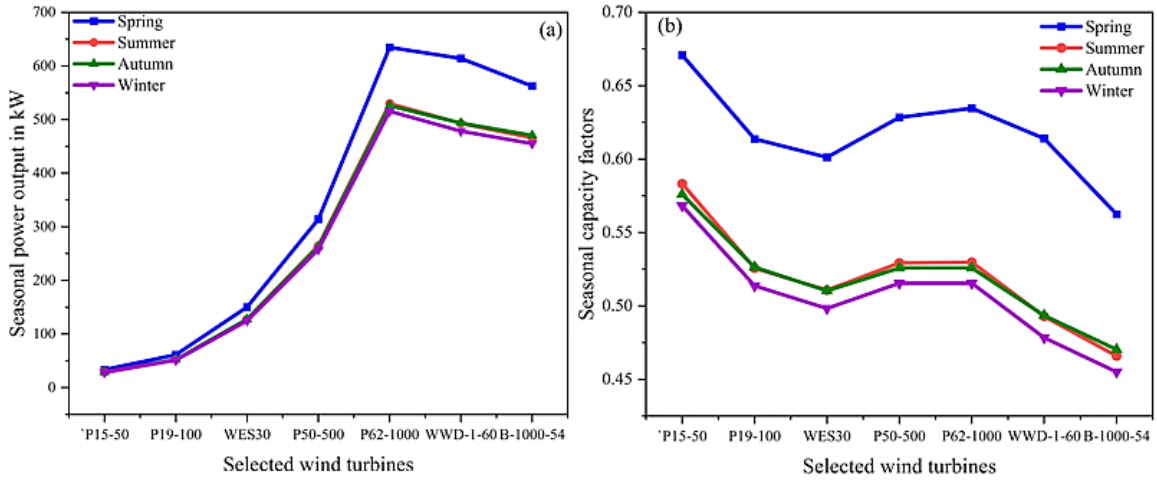


**Figure 8. Seasonal (a) Turbine power output and (b) Performance of the turbines**

### 5.7.2. Monthly Wind Turbine Performance Analysis

The monthly performance analysis of the selected WT models revealed varying power intervals from January-December. The POLARIS P15-50 WT had a power range of 32.477–42.365 kW, while the power range of the POLARIS P19-100 was 4.78–7.689 kW. The WES30 and POLARIS P50-500 WTs fell within the medium power range, generating 136.12–190.42 kW and 245.46–401.23 kW, respectively. The remaining WT models exhibited a higher AP than the others. The POLARIS P62-1000 had the largest AP (541.86–808.63 kW), followed by the WWD-1-60 and BONUS B-1000-54 (466.39–792.71 kW and 437.42–714.28 kW, respectively). The highest AP for all the WTs was in March (7.689–808.632 kW), followed by January (6.879–724.716 kW). The other months exhibited power ranging from 4.78–

724.819 kW (Table 6). Consequently, the WT model with the highest monthly power generation was the POLARIS P62-1000, which was capable of producing power that was comparable to that generated by other WT models within the range of 541.86–808.63 kW.

**Table 6. Monthly average power (kW) output of the selected wind turbine models**

| Months | `P15-50 | P19-100 | WES30 | P50-500 | P62-1000 | WWD-1-60 | B-1000-54 |
|---|---|---|---|---|---|---|---|
| 1 | 38.221 | 6.879 | 169.840 | 358.949 | 724.716 | 706.035 | 634.353 |
| 2 | 33.616 | 6.032 | 148.656 | 315.903 | 639.739 | 617.350 | 554.778 |
| 3 | 42.365 | 7.689 | 190.423 | 401.233 | 808.632 | 792.711 | 714.280 |
| 4 | 35.495 | 6.691 | 162.195 | 319.003 | 622.116 | 596.106 | 601.972 |
| 5 | 30.095 | 5.596 | 136.121 | 274.226 | 541.863 | 518.397 | 506.262 |
| 6 | 32.477 | 5.780 | 142.724 | 306.866 | 624.786 | 602.521 | 532.569 |
| 7 | 34.226 | 5.739 | 142.951 | 324.837 | 676.981 | 667.561 | 525.605 |
| 8 | 34.003 | 6.078 | 149.976 | 320.104 | 649.508 | 628.058 | 559.633 |
| 9 | 33.814 | 5.731 | 142.636 | 321.422 | 667.717 | 656.105 | 526.715 |
| 10 | 26.131 | 4.780 | 117.055 | 245.463 | 494.339 | 466.392 | 437.422 |
| 11 | 34.207 | 6.260 | 153.356 | 316.635 | 632.705 | 608.967 | 571.764 |
| 12 | 38.112 | 6.841 | 169.014 | 358.430 | 724.819 | 706.620 | 631.180 |

Table 7 presents the monthly CP values. The results indicated that the largest monthly CP was achieved using the POLARIS 15-50 WT (52.226–84.73%). However, it had the smallest AP. The CP of the POLARIS P62-1000 ranged from 49.43–80.8%, followed by the POLARIS P50-500 (49.09–80.25%). The WWD-1-60 WT exhibited a CP ranging between 46.64–79.27%. All the WTs demonstrated a CP of > 25%, indicating their cost-effectiveness. Among these models, the POLARIS P62-1000 stood out as the WT with the best performance for installation at the site. The month with the largest CP was March (71.43–84.73%), followed by January (63.44–76.6%). This means that all the selected WTs had CP values within those ranges in January and March, while in the other months CP values ranged between 43.74–79.27%. In general, the CP for of all the months was > 25%. This means that all the WTs were cost-effective for all the months, and hence, the site had good wind regimes.

It has been proven that all seven WTs were cost-effective, but the most highly efficient WTs were the P62-1000, WWD-1-60, B-1000-54, and P50-500 due to their height and rotor diameter. The height and rotor diameter of a WT significantly impact its performance in converting WP into electrical power. Taller WTs benefit from higher WSs, reduced turbulence, and access to more consistent wind resources at greater heights. However, taller towers entail increased construction costs. The heights of the first three high-performance WTs, namely the P62-1000, WWD-1-60, and B-1000-54, were 60, 70, 45, and 50 m, respectively, while the other WTs had heights ranging between 30–36 m. Also, rotors with larger diameters are able to capture more WP, thus improving power output and efficiency, especially at lower WSs, as depicted in this research for the first four high-performance WTs, which had blade diameters of between 50–62 m. Despite a higher initial investment in taller towers and larger rotor diameters, enhanced energy production often justifies these costs, particularly in regions with lower WSs. Therefore, the P62-1000 was chosen as the high-performance WT for the site. Nevertheless, since all the WTs were cost-effective on an annual, seasonal, and monthly basis, any of the WTs analyzed in this research can be selected based on the investment budget or cost benefit of the investment plan.

**Table 7. Monthly Performance of the wind turbine models**

| Months | `P15-50 | P19-100 | WES30 | P50-500 | P62-1000 | WWD-1-60 | B-1000-54 |
|---|---|---|---|---|---|---|---|
| 1 | 0.7644 | 0.6879 | 0.6794 | 0.7179 | 0.7247 | 0.7060 | 0.6344 |
| 2 | 0.6723 | 0.6032 | 0.5946 | 0.6318 | 0.6397 | 0.6174 | 0.5548 |
| 3 | 0.8473 | 0.7689 | 0.7617 | 0.8025 | 0.8086 | 0.7927 | 0.7143 |
| 4 | 0.7099 | 0.6691 | 0.6488 | 0.6380 | 0.6221 | 0.5961 | 0.6020 |
| 5 | 0.6019 | 0.5596 | 0.5445 | 0.5485 | 0.5419 | 0.5184 | 0.5063 |
| 6 | 0.6495 | 0.5780 | 0.5709 | 0.6137 | 0.6248 | 0.6025 | 0.5326 |
| 7 | 0.6845 | 0.5739 | 0.5718 | 0.6497 | 0.6770 | 0.6676 | 0.5256 |
| 8 | 0.6801 | 0.6078 | 0.5999 | 0.6402 | 0.6495 | 0.6281 | 0.5596 |
| 9 | 0.6763 | 0.5731 | 0.5705 | 0.6428 | 0.6677 | 0.6561 | 0.5267 |
| 10 | 0.5226 | 0.4780 | 0.4682 | 0.4909 | 0.4943 | 0.4664 | 0.4374 |
| 11 | 0.6841 | 0.6260 | 0.6134 | 0.6333 | 0.6327 | 0.6090 | 0.5718 |
| 12 | 0.7622 | 0.6841 | 0.6761 | 0.7169 | 0.7248 | 0.7066 | 0.6312 |

## 6. Discussion

The scientific findings from the analysis of the wind data at the study site in Zanzibar revealed several important insights regarding wind characteristics and their implications for WP generation. Firstly, the site experienced a consistent daily average WS from 05:00–20:00 across all seasons, peaking at approximately 7 m/s at 15:00 and gradually decreasing to 4 m/s by 23:00. This consistent and sustainable wind profile indicates a favorable environment for WP generation throughout the day, providing a reliable source of renewable energy. Furthermore, the monthly, seasonal, and annual *k* and *c* factors indicated strong and sustainable wind conditions, which are conducive to energy generation. With a *k* factor of > 1.54 and a *c* factor of > 9 m/s, the wind characteristics at the site fell within the super-exponential margin, highlighting the potential for robust WP generation. The results of the analysis also revealed that the most frequent WSs of > 4.5 m/s were experienced over 80% of all the months, further emphasizing the substantial WP potential at the study site.

Also, the monthly wPD ranged between 459.886–7048.452 W/m$^2$, and the seasonal WP ranged between 1500–11000 W/m$^2$, while the annual wED was > 13.52 GWh/m$^2$, demonstrating the variability in WP potential across different months. Based on the NREL classification of WP, the wED of the site ranged between Class 3 (Decent class) to Class 7 (Superb class). Moreover, the performance evaluation of the seven WT models demonstrated that all the analyzed WTs exceeded their rated power output, indicating their suitability for installation in the region. Although the POLARIS P62-1000 emerged as the most effective WT model, the selection of the WT model can be based on project budget considerations, as each model offers distinct parameters such as tower height and rotor diameter. Overall, these findings underscored the feasibility and effectiveness of harnessing WP in Zanzibar, with implications for sustainable energy production and potential WT selection for WP projects.

In comparison to some previous study sites, the study site for this research appeared to have sufficient and sustainable wind resources at a height of 10 m. For example, a study conducted in the Kingdom of Bahrain [31] analyzed data on hourly measurements of WS collected between 2003–2005 at a height of 10 m. The findings revealed significant variations in wED throughout the year, with the maximum wED recorded in February at 10 m being 164.33 W/m$^2$, while the minimum wED was observed in October (65.33 W/m$^2$). The average annual wPD calculated at a height of 10 m was 114.54 W/m$^2$. These findings provided valuable insights into the WP potential and variability in wPD at a height of 10 m in Bahrain, which are essential for the optimal planning and deployment of WP projects in the region. Due to the results of the study in Bahrain, Zanzibar shows a more competitive advantage because, at the same height of 10 m, Zanzibar seems to have higher WS variations and WP densities.

Also, compared to the evaluation of the technical WP potential of the Kiisi region [24], Zanzibar still has the advantage of feasible wind resources. For example, the findings on the Kiisi region revealed a WS frequency distribution of 2.9 m/s with an SD of 1.5 at 10 m, while regional variations in WSs are assessed through the calculation of averages at different hub heights. Moreover, the study determined that the mean wPD is 29 W/m$^2$ for the region, with the Rayleigh model having a slightly smaller wED as compared to that at the site of this study. The observations show a gradual decline in WSs over the years, making the site marginally suitable for WP generation but still viable for non-grid connected applications.

In the coastal region of Dar es Salaam [38], the average monthly WS fluctuates between 4.56–6.09 m/s. However, the monthly WP densities exhibit a wider range (36–139 W/m$^2$) at 10 m, which is too small compared to the results of the wPD of the study site for this research. The lower WS and WP observed in some months can be attributed to local influences, particularly human activities such as urbanization, land use changes, and the construction of buildings and infrastructure. These factors alter local wind patterns, introducing obstacles and surface roughness that disrupt wind flow and diminish the WP potential. Despite these challenges, the study identified the P50–500 WT as being the most suitable for the site. This preference is justified by its highest CP and substantial power output compared to the other evaluated WTs.

This research utilized half-hourly wind data collected throughout 2022 at a consistent height of 10 m along the coastal region of Zanzibar. This extensive dataset provides a detailed understanding of wind characteristics and patterns over an extended period of time, enhancing the robustness and reliability of the findings. The assessment of WP potential was restricted to a height of 10 m, thus overlooking the potential impact of extrapolating power and energy potential at different heights. Future studies at the study site of this research should consider extrapolating data from multiple heights to provide a more comprehensive understanding of the availability of wind resources and optimize the siting of WTs for enhanced energy generation efficiency.

## 7. Conclusion

In this research, a comprehensive analysis was conducted of the monthly and seasonal WP potential and performance of selected WT models. The results will enable researchers, energy investment organizations, and policymakers to understand the WP resources at the study site. Also, it is a starting point for future studies by filling in the limitations of this research. The study used data collected twice hourly for a full year (2022) along the coast of Zanzibar at a height of 10 m above ground. Future wind analysis studies at the site are expected to extend the dataset up to five recent years and consider an extrapolation of WS and power at different heights to gain a broader knowledge of wind patterns at the site.

The results showed that the site has sustainable WSs and significant energy potential, meeting the criteria for classification as a Class 7, according to NREL standards. The annual wED was >13.52 GWh/m$^2$, the monthly AP was 1300–7100 kW/m$^2$ for more than nine months, with the AP for the remaining two months ranging from 460–950 kW/m$^2$. The assessment of the monthly and seasonal AP and CP indicated good wind patterns at the study site, with all the WT models exhibiting a CP of > 25%. The POLARIS P62-1000 WT stands out as a highly recommended model due to its consistent demonstration of the largest AP and CP across annual and seasonal considerations. However, all the selected WTs are deemed to be cost-effective, providing viable options for harnessing WP at the site, according to the investment budget and targeted output.

This article contributes new knowledge in the domain of WP by conducting a comprehensive analysis of monthly and seasonal WP potential and WT performance. It established the fact that the study site possesses sustainable WSs and significant energy potential, meeting NREL classification standards. The research demonstrated the cost-effectiveness of various WT models, all of which exhibited a CP of > 25%, providing viable options for WP harnessing.

## 8. Nomenclatures

| | | | |
|---|---|---|---|
| $C_f$ | Capacity factor of the turbine | E | Wind energy density in kWh/m$^2$ |
| P | Wind power density in W/m$^2$ | $\bar{v}$ | Mean wind speed in m/s |
| $v_m$ | Maximum wind speed in m/s | $v_p$ | Likely wind speed in m/s |
| $v_c$ | Starting speed of the wind turbine | $v_f$ | Ceasing speed of the wind turbine |
| $v_r$ | Nominal speed of the wind turbine | $P_e$ | Average power of the wind turbine |
| $P_R$ | Nominal power of the wind turbine | $\rho$ | Atmospheric density (1.225 kg/m$^3$) |
| AP | Average Power | CP | Capacity Factor |
| wED | Wind Energy Density | WD | Weibull Distribution |
| WP | Wind Power | PD | Power Density |
| WT | Wind Turbine | | |

## 9. Declarations

### 9.1. Author Contributions

Conceptualization, D.D.D.P.T. and U.; methodology, B.H.S., D.D.D.P.T., and U.; software, B.H.S.; validation, B.H.S., D.D.D.P.T., and U.; formal analysis, B.H.S., D.D.D.P.T., and U.; investigation, B.H.S., D.D.D.P.T., U., M.A., and M.T.M.; resources, D.D.D.P.T. and U.; data curation, B.H.S., D.D.D.P.T., and U.; writing—original draft preparation, B.H.S.; writing—review and editing, B.H.S., D.D.D.P.T., U., M.A., and M.T.M.; visualization, B.H.S.; supervision, D.D.D.P.T. and U.; project administration, D.D.D.P.T. and U.; funding acquisition, U. All authors have read and agreed to the published version of the manuscript.

### 9.2. Data Availability Statement

The data presented in this study are available in the article.

### 9.3. Funding

This research was supported by Universitas Sebelas Maret-Year 2024 Under research scheme of "Penelitian kolaborasi Internasional (KI-UNS) with financial aid of HIBAH non APBN, and contract number 194.2/UNS27.22/PT.01.03/2024.

### 9.4. Acknowledgements

The authors of this research highly acknowledge Graduate School of Engineering Faculty of the Sebelas Maret University for all support, including instructive and financial acquisition from the initial to the final stage of this research.

### 9.5. Institutional Review Board Statement

Not applicable.

### 9.6. Informed Consent Statement

Not applicable.

### 9.7. Declaration of Competing Interest

The authors declare that they have no known competing financial interests or personal relationships that could have appeared to influence the work reported in this paper.

## 10. References

[1] Prihantini, N. B., Rakhmayanti, N., Handayani, S., Sjamsuridzal, W., Wardhana, W., & Nasruddin. (2020). Biomass production of indonesian indigenous leptolyngbya strain on NPK fertilizer medium and its potential as a source of biofuel. Evergreen, 7(4), 593–601. doi:10.5109/4150512.

[2] Furutani, Y., Norinaga, K., Kudo, S., Hayashi, J. I., & Watanabe, T. (2017). Current situation and future scope of biomass gasification in Japan. Evergreen, 4(4), 24–29. doi:10.5109/1929681.

[3] Jhalani, A., Agarwal, A., Singh, D., & Sharma, S. (2023). Energy Security Scenarios for India Under Diversified Demand and Supply. Evergreen, 10(4), 2683–2689. doi:10.5109/7160927.

[4] Mirza, F. M., & Kanwal, A. (2017). Energy consumption, carbon emissions and economic growth in Pakistan: Dynamic causality analysis. Renewable and Sustainable Energy Reviews, 72, 1233–1240. doi:10.1016/j.rser.2016.10.081.

[5] Bogner, J., Pipatti, R., Hashimoto, S., Diaz, C., Mareckova, K., Diaz, L., Kjeldsen, P., Monni, S., Faaij, A., Qingxian, G., Tianzhu, Z., Mohammed, A. A., Sutamihardja, R. T. M., & Gregory, R. (2008). Mitigation of global greenhouse gas emissions from waste: Conclusions and strategies from the Intergovernmental Panel on Climate Change (IPCC) Fourth Assessment Report. Working Group III (Mitigation). Waste Management and Research, 26(1), 11–32. doi:10.1177/0734242X07088433.

[6] Surendra, K. C., Takara, D., Hashimoto, A. G., & Khanal, S. K. (2014). Biogas as a sustainable energy source for developing countries: Opportunities and challenges. Renewable and Sustainable Energy Reviews, 31, 846–859. doi:10.1016/j.rser.2013.12.015.

[7] Pan, S. Y., Gao, M., Kim, H., Shah, K. J., Pei, S. L., & Chiang, P. C. (2018). Advances and challenges in sustainable tourism toward a green economy. Science of the Total Environment, 635, 452–469. doi:10.1016/j.scitotenv.2018.04.134.

[8] Kuriqi, A., Pinheiro, A. N., Sordo-Ward, A., Bejarano, M. D., & Garrote, L. (2021). Ecological impacts of run-of-river hydropower plants—Current status and future prospects on the brink of energy transition. Renewable and Sustainable Energy Reviews, 142. doi:10.1016/j.rser.2021.110833.

[9] Mukimin, A., & Vistanty, H. (2023). Low carbon development based on microbial fuel cells as electrical generation and wastewater treatment unit. Renewable Energy Focus, 44, 132–138. doi:10.1016/j.ref.2022.12.005.

[10] Alias, N. D., & Go, Y. I. (2023). Decommissioning platforms to offshore solar system: Road to green hydrogen production from seawater. Renewable Energy Focus, 46, 136–155. doi:10.1016/j.ref.2023.05.003.

[11] Kuncoro, A., & Purwanto, W. W. (2020). Analysis of energy-water nexus palm oil biodiesel production in Riau using life cycle assessment and water footprint methods. Evergreen, 7(1), 104–110. doi:10.5109/2740965.

[12] Wang, J., & Dong, K. (2019). What drives environmental degradation? Evidence from 14 Sub-Saharan African countries. Science of the Total Environment, 656, 165–173. doi:10.1016/j.scitotenv.2018.11.354.

[13] Ahlborg, H., & Hammar, L. (2014). Drivers and barriers to rural electrification in Tanzania and Mozambique - grid-extension, off-grid, and renewable energy technologies. Renewable Energy, 61, 117–124. doi:10.1016/j.renene.2012.09.057.

[14] Mofijur, M., Masjuki, H. H., Kalam, M. A., Hazrat, M. A., Liaquat, A. M., Shahabuddin, M., & Varman, M. (2012). Prospects of biodiesel from Jatropha in Malaysia. Renewable and Sustainable Energy Reviews, 16(7), 5007–5020. doi:10.1016/j.rser.2012.05.010.

[15] Soemanto, A., Mohi, E., al Irsyad, M. I., & Gunawan, Y. (2023). The Role of Oil Fuels on the Energy Transition toward Net Zero Emissions in Indonesia: A Policy Review. Evergreen 10(4), 2074–2083. doi:10.5109/7160867.

[16] Bansal, M., Agarwal, A., Pant, M., & Kumar, H. (2021). Challenges and opportunities in energy transformation during COVID-19. Evergreen 8(2), 255–261. doi:10.5109/4480701.

[17] Eberhard, A., Gratwick, K., Morella, E., & Antmann, P. (2017). Independent Power Projects in Sub-Saharan Africa: Investment trends and policy lessons. Energy Policy, 108(August 2016), 390–424. doi:10.1016/j.enpol.2017.05.023.

[18] Ulsrud, K., Winther, T., Palit, D., & Rohracher, H. (2015). Village-level solar power in Africa: Accelerating access to electricity services through a socio-technical design in Kenya. Energy Research and Social Science, 5, 34–44. doi:10.1016/j.erss.2014.12.009.

[19] Ismaiel, A. M. M., Metwalli, S. M., Elhadidi, B. M. N., & Yoshida, S. (2017). Fatigue analysis of an optimized HAWT composite blade. Evergreen, 4(2–3), 1–6. doi:10.5109/1929656.

[20] Franco, A., Shaker, M., Kalubi, D., & Hostettler, S. (2017). A review of sustainable energy access and technologies for healthcare facilities in the Global South. Sustainable Energy Technologies and Assessments, 22, 92–105. doi:10.1016/j.seta.2017.02.022.

[21] Li, C., & Ito, K. (2014). Performance evaluation of wind decontamination system by computational fluid dynamics. Evergreen, 1(2), 12–17. doi:10.5109/1495158.

[22] Takeyeldein, M. M., Lazim, T. M., Ishak, I. S., Nik Mohd, N. A. R., & Ali, E. A. (2020). Wind lens performance investigation at low wind speed. Evergreen, 7(4), 481–488. doi:10.5109/4150467.

[23] Ashwindran, S. N., Azizuddin, A. A., & Oumer, A. N. (2021). Study of √2 conjecture in the construction of drag induced wind turbine blade morphology. Evergreen, 8(3), 574–585. doi:10.5109/4491649.

[24] Ongaki, N. L., Maghanga, C. M., & Kerongo, J. (2021). Evaluation of the Technical Wind Energy Potential of Kisii Region Based on the Weibull and Rayleigh Distribution Models. Journal of Energy, 2021, 1–17. doi:10.1155/2021/6627509.

[25] Topaloğlu, F., & Pehlivan, H. (2018). Analysis of Wind Data, Calculation of Energy Yield Potential, and Micrositing Application with WAsP. Advances in Meteorology, 2018. doi:10.1155/2018/2716868.

[26] Narula, K. (2019). Energy security and sustainability. Lecture Notes in Energy, 68(1), 3–22. doi:10.1007/978-981-13-1589-3_1.

[27] Keyhani, A., Ghasemi-Varnamkhasti, M., Khanali, M., & Abbaszadeh, R. (2010). An assessment of wind energy potential as a power generation source in the capital of Iran, Tehran. Energy, 35(1), 188–201. doi:10.1016/j.energy.2009.09.009.

[28] Wang, Z., Wang, X., & Liu, W. (2023). Genetic least square estimation approach to wind power curve modelling and wind power prediction. Scientific Reports, 13(1), 1–15. doi:10.1038/s41598-023-36458-w.

[29] Babu, V. V., Preetha Roselyn, J., & Sundaravadivel, P. (2023). Multi-objective genetic algorithm-based energy management system considering optimal utilization of grid and degradation of battery storage in microgrid. Energy Reports, 9, 5992–6005. doi:10.1016/j.egyr.2023.05.067.

[30] Chirwa, D., Goyal, R., & Mulenga, E. (2023). Floating solar photovoltaic (FSPV) potential in Zambia: Case studies on six hydropower power plant reservoirs. Renewable Energy Focus, 44, 344–356. doi:10.1016/j.ref.2023.01.007.

[31] Jowder, F. A. L. (2009). Wind power analysis and site matching of wind turbine generators in Kingdom of Bahrain. Applied Energy, 86(4), 538–545. doi:10.1016/j.apenergy.2008.08.006.

[32] Awad, M. M. (2013). Comments on "assessment of different methods used to estimate Weibull distribution parameters for wind speed in Zafarana wind farm, Suez Gulf, Egypt." Energy, 58, 714. doi:10.1016/j.energy.2013.06.034.

[33] Celik, A. N. (2003). Energy output estimation for small-scale wind power generators using Weibull-representative wind data. Journal of Wind Engineering and Industrial Aerodynamics, 91(5), 693–707. doi:10.1016/S0167-6105(02)00471-3.

[34] Katinas, V., Gecevicius, G., & Marciukaitis, M. (2018). An investigation of wind power density distribution at location with low and high wind speeds using statistical model. Applied Energy, 218, 442–451. doi:10.1016/j.apenergy.2018.02.163.

[35] Katinas, V., Marčiukaitis, M., Gecevičius, G., & Markevičius, A. (2017). Statistical analysis of wind characteristics based on Weibull methods for estimation of power generation in Lithuania. Renewable Energy, 113, 190–201. doi:10.1016/j.renene.2017.05.071.

[36] Sukkiramathi, K., & Seshaiah, C. V. (2020). Analysis of wind power potential by the three-parameter Weibull distribution to install a wind turbine. Energy Exploration and Exploitation, 38(1), 158–174. doi:10.1177/0144598719871628.

[37] Luankaeo, S., & Tirawanichakul, Y. (2017). Assessment of Wind Energy Potential in Prince of Songkla University (South Part of Thailand): Hatyai campus. Energy Procedia, 138, 704–709. doi:10.1016/j.egypro.2017.10.204.

[38] Michael, E., Tjahjana, D. D. D. P., & Prabowo, A. R. (2021). Estimating the potential of wind energy resources using Weibull parameters: A case study of the coastline region of Dar es Salaam, Tanzania. Open Engineering 11(1), 1093–1104. doi:10.1515/eng-2021-0108.

[39] Oyedepo, S. O., Adaramola, M. S., & Paul, S. S. (2012). Analysis of wind speed data and wind energy potential in three selected locations in South-East Nigeria. International Journal of Energy and Environmental Engineering, 3(1), 1–11. doi:10.1186/2251-6832-3-7.

[40] Gagliano, A., Nocera, F., Patania, F., & Capizzi, A. (2013). Assessment of micro-wind turbines performance in the urban environments: An aided methodology through geographical information systems. International Journal of Energy and Environmental Engineering, 4(1), 1–14. doi:10.1186/2251-6832-4-43.

[41] Fyrippis, I., Axaopoulos, P. J., & Panayiotou, G. (2010). Wind energy potential assessment in Naxos Island, Greece. Applied Energy, 87(2), 577–586. doi:10.1016/j.apenergy.2009.05.031.

[42] Pellegrini, L., & Tasciotti, L. (2013). Rural electrification now and then: Comparing contemporary challenges in developing countries to the USA's experience in retrospect. Forum for Development Studies, 40(1), 153–176. doi:10.1080/08039410.2012.732108.

[43] Aly, A., Jensen, S. S., & Pedersen, A. B. (2017). Solar power potential of Tanzania: Identifying CSP and PV hot spots through a GIS multicriteria decision making analysis. Renewable Energy, 113, 159–175. doi:10.1016/j.renene.2017.05.077.

[44] Trotter, P. A., McManus, M. C., & Maconachie, R. (2017). Electricity planning and implementation in sub-Saharan Africa: A systematic review. Renewable and Sustainable Energy Reviews, 74, 1189–1209. doi:10.1016/j.rser.2017.03.001.

[45] Pishgar-Komleh, S. H., Keyhani, A., & Sefeedpari, P. (2015). Wind speed and power density analysis based on Weibull and Rayleigh distributions (a case study: Firouzkooh county of Iran). Renewable and Sustainable Energy Reviews, 42, 313–322. doi:10.1016/j.rser.2014.10.028.

[46] Werapun, W., Tirawanichakul, Y., & Waewsak, J. (2015). Comparative Study of Five Methods to Estimate Weibull Parameters for Wind Speed on Phangan Island, Thailand. Energy Procedia, 79. doi:10.1016/j.egypro.2015.11.596.

[47] Al-Ghriybah, M. (2022). Assessment of Wind Energy Potentiality at Ajloun, Jordan Using Weibull Distribution Function. Evergreen, 9(1), 10–16. doi:10.5109/4774211.

[48] Patrai, K., & Gupta, S. (2023). Reliability Estimation of a Degradable System using Intuitionistic Fuzzy Weibull Lifetime Distribution. Evergreen, 10(4), 2317–2324. doi:10.5109/7160909.

[49] Ali, S., Lee, S. M., & Jang, C. M. (2018). Statistical analysis of wind characteristics using Weibull and Rayleigh distributions in Deokjeok-do Island – Incheon, South Korea. Renewable Energy, 123, 652–663. doi:10.1016/j.renene.2018.02.087.

[50] Akpinar, E. K., & Akpinar, S. (2005). An assessment on seasonal analysis of wind energy characteristics and wind turbine characteristics. Energy conversion and management, 46(11-12), 1848-1867. doi:10.1016/j.enconman.2004.08.012.

[51] Mahmood, F. H., Resen, A. K., & Khamees, A. B. (2020). Wind characteristic analysis based on Weibull distribution of Al-Salman site, Iraq. Energy Reports, 6(September 2019), 79–87. doi:10.1016/j.egyr.2019.10.021.

[52] Chang, T. P. (2011). Performance comparison of six numerical methods in estimating Weibull parameters for wind energy application. Applied Energy, 88(1), 272–282. doi:10.1016/j.apenergy.2010.06.018.

[53] MERT, İ., & KARAKUŞ, C. (2015). A statistical analysis of wind speed data using Burr, generalized gamma, and Weibull distributions in Antakya, Turkey. Turkish Journal of Electrical Engineering & Computer Sciences, 23(6), 1571–1586. doi:10.3906/elk-1402-66.

[54] Guarienti, J. A., Kaufmann Almeida, A., Menegati Neto, A., de Oliveira Ferreira, A. R., Ottonelli, J. P., & Kaufmann de Almeida, I. (2020). Performance analysis of numerical methods for determining Weibull distribution parameters applied to wind speed in Mato Grosso do Sul, Brazil. Sustainable Energy Technologies and Assessments, 42, 100854. doi:10.1016/j.seta.2020.100854.

[55] Alanazi, M. A., Aloraini, M., Islam, M., Alyahya, S., & Khan, S. (2023). Wind energy assessment using Weibull distribution with different numerical estimation methods: a case study. Emerging Science Journal, 7(6), 2260-2278. doi:10.28991/ESJ-2023-07-06-024.

[56] Wang, Z., & Liu, W. (2021). Wind energy potential assessment based on wind speed, its direction and power data. Scientific Reports, 11(1), 1–15. doi:10.1038/s41598-021-96376-7.

[57] Chang, T. P. (2011). Estimation of wind energy potential using different probability density functions. Applied Energy, 88(5), 1848–1856. doi:10.1016/j.apenergy.2010.11.010.

[58] Eriksson, S., Bernhoff, H., & Leijon, M. (2008). Evaluation of different turbine concepts for wind power. Renewable and Sustainable Energy Reviews, 12(5), 1419–1434. doi:10.1016/j.rser.2006.05.017.

[59] Ajayi, O. O., Fagbenle, R. O., Katende, J., Aasa, S. A., & Okeniyi, J. O. (2013). Wind profile characteristics and turbine performance analysis in Kano, north-western Nigeria. International Journal of Energy and Environmental Engineering, 4(1), 1–15. doi:10.1186/2251-6832-4-27.

[60] Daoudi, M., Abdelaziz, A. S. M., Mohammed, E., & Elmostapha, E. (2019). Wind speed data and wind energy potential using weibull distribution in zagora, morocco. International Journal of Renewable Energy Development, 8(3), 267–273. doi:10.14710/ijred.8.3.267-273.

[61] Filom, S., Radfar, S., Panahi, R., Amini, E., & Neshat, M. (2021). Exploring wind energy potential as a driver of sustainable development in the southern coasts of Iran: The importance of wind speed statistical distribution model. Sustainability (Switzerland), 13(14), 7702. doi:10.3390/su13147702.